



Advances in Water in Agrosience

Fitting a numerical model for the analysis of wet bulb dimensions by drip irrigation

Ajuste de un modelo numérico para el análisis de las dimensiones del bulbo húmedo bajo riego por goteo

Ajuste de um modelo numérico para a análise das dimensões do bulbo molhado sob irrigação por gotejamento

Sastre, M. T. ¹; Silveira, L. ¹; Gamazo, P. ²

¹Universidad de la República, Facultad de Ingeniería, Instituto de Mecánica de los Fluidos e Ingeniería Ambiental, Montevideo, Uruguay

²Universidad de la República, Centro Universitario Regional Litoral Norte, Departamento del Agua, Salto, Uruguay

Editor

Lucía Puppo 
Universidad de la República, Montevideo,
Uruguay

Received 28 Apr 2023

Accepted 21 Aug 2023

Published 06 Feb 2024

Correspondence

Pablo Gamazo
pablogamazo@gmail.com

Abstract

Drip irrigation is globally acknowledged as the most efficient system. However, the concept of "efficiency" relies on irrigation cultural practices, local agro-climatic conditions, and soil characteristics. In Uruguay, the absence of accurate wet bulb shape prediction often leads to common over-irrigation practices. Consequently, water loss through deep percolation, groundwater contamination, reduced crop yields, higher energy expenditure, and elevated fertilizer usage introduce uncertainties about the true efficiency of drip irrigation. The primary objective of this study is to develop a methodology for estimating wet bulb dimensions and their dynamics under drip irrigation. To achieve this, an experiment was conducted using a lysimeter containing representative soil from southern Uruguay. Alfalfa was irrigated using a central dripper with varying application times and flow rates. The lysimeter was equipped with tensiometers, and moisture observations were made with a neutron probe. The collected data were used to calibrate a numerical model implemented in the Code Bright program (UPC, Barcelona, Spain). The model exhibited a good fit in the upper strata ($h < 60\text{cm}$), and revealed a deeper and thinner bulb compared to estimates found in the literature for soils of similar texture. This model, accurately computing the wet bulb's shape in heavy and stratified soils in Uruguay, allows simulations of various irrigation scenarios. Consequently, this work holds great potential for improving the efficiency of drip irrigation in the region.

Keywords: drip dynamics, drip irrigation, clay soils, numerical modeling, wet bulb

Resumen

El riego por goteo es reconocido mundialmente como el sistema más eficiente. Sin embargo, el concepto de *eficiencia* se basa en las prácticas culturales de riego, las condiciones agroclimáticas locales y las características del suelo. En Uruguay, la ausencia de una predicción precisa de la forma del bulbo húmedo a menudo conduce a prácticas comunes de riego excesivo. En consecuencia, la pérdida de agua a través de la percolación profunda, la contaminación de las aguas subterráneas, la reducción del rendimiento de los cultivos, el mayor gasto de energía y el uso elevado de fertilizantes introducen incertidumbres sobre la verdadera eficiencia del riego por goteo. El objetivo principal de este estudio es desarrollar una metodología para estimar las dimensiones del bulbo húmedo y su dinámica bajo riego por goteo. Para lograr esto, se realizó un experimento utilizando un lisímetro que contenía suelo representativo del sur de Uruguay. La alfalfa se



regó con un gotero central con diferentes tiempos de aplicación y caudales. El lisímetro estaba equipado con tensiómetros y las observaciones de humedad se realizaron con una sonda de neutrones. Los datos recopilados se utilizaron para calibrar un modelo numérico implementado en el programa Code Bright (UPC, Barcelona, España). El modelo exhibió un buen ajuste en los estratos superiores ($h < 60\text{cm}$) y reveló un bulbo más profundo y delgado en comparación con las estimaciones encontradas en la literatura para suelos de textura similar. Este modelo, que calcula con precisión la forma del bulbo húmedo en suelos pesados y estratificados en Uruguay, permite simulaciones de varios escenarios de riego. En consecuencia, este trabajo tiene un gran potencial para mejorar la eficiencia del riego por goteo en la región.

Palabras clave: dinámica de goteo, riego por goteo, suelos arcillosos, modelado numérico, bulbo húmedo

Resumo

A irrigação por gotejamento é mundialmente reconhecida como o sistema mais eficiente. No entanto, o conceito de "eficiência" depende de práticas culturais de irrigação, condições agroclimáticas locais e características do solo. No Uruguai, a ausência de previsão precisa da forma do bulbo úmido geralmente leva a práticas comuns de irrigação excessiva. Consequentemente, a perda de água por percolação profunda, contaminação de águas subterrâneas, rendimentos reduzidos das culturas, maior gasto de energia e uso elevado de fertilizantes introduzem incertezas sobre a verdadeira eficiência da irrigação por gotejamento. O objetivo principal deste estudo é desenvolver uma metodologia para estimar as dimensões do bulbo úmido e sua dinâmica sob irrigação por gotejamento. Para isso, foi realizado um experimento utilizando um lisímetro contendo solo representativo do sul do Uruguai. A alfafa foi irrigada usando um gotejador central com diferentes tempos de aplicação e vazões. O lisímetro foi equipado com tensiómetros e as observações de umidade foram feitas com uma sonda de nêutrons. Os dados coletados foram usados para calibrar um modelo numérico implementado no programa Code Bright (UPC, Barcelona, Espanha). O modelo apresentou um bom ajuste nos estratos superiores ($h < 60\text{cm}$) e revelou um bulbo mais profundo e mais fino em relação às estimativas encontradas na literatura para solos de textura semelhante. Este modelo, calculando com precisão a forma do bulbo úmido em solos pesados e estratificados no Uruguai, permite simulações de vários cenários de irrigação. Consequentemente, este trabalho tem grande potencial para melhorar a eficiência da irrigação por gotejamento na região.

Palavras-chave: dinâmica de gotejamento, irrigação por gotejamento, solos argilosos, modelagem numérica, bulbo úmido

1. Introduction

In several countries, such as Uruguay, there are agricultural areas with high land value and small-scale producers. When climatic conditions with high inter-annual variability exist, production is affected, and farmers can only grow by increasing productivity through the use of efficient irrigation techniques. In Uruguay, a large part of fruit and vegetable production is carried out under drip irrigation.

It is globally technically acknowledged that drip irrigation is the most efficient system, registering efficiencies between 60% and 95%⁽¹⁾. However, from the 1990s onwards the absolute affirmation of efficiency and advantages such as the non-existence of deep percolation have been questioned by several authors and begin to be conditioned to the design and its management⁽²⁻⁸⁾. These authors claim that the method is efficient only if the design and operation are based on a good estimation of the shape and dimensions of the wet bulb, since plants do not respond directly to the frequency of water application, but to the water potential (tension) in the soil.

In the last 30 years, great advances have been made in the implementation of drip irrigation techniques. Most of the research focuses on particular

experiences with certain soil types, crops and irrigation designs, which are not very generalizable⁽⁷⁻¹⁰⁾.

Regarding Uruguay, there is not enough research data about soil characterization, agro-climatic variables and statistics to allow a correct design of drip irrigation. These factors are considered without taking into account the local conditions of the soil-water-plant system. In general, experiences and data from other regions, such as Europe and the US, are adopted. Drip irrigation has a strong experimental basis in arid and semi-arid climates, light and homogeneous soils, those in which it was developed. However, García Petillo⁽¹¹⁾ points out that the claim of greater efficiency and greater water savings does not always have sufficient experimental basis for conditions other than those in which drip irrigation was developed. In fact, the experience in Uruguay seems to indicate that the efficiencies are not such due to deep percolation and soil compaction phenomena. According to García Petillo⁽¹²⁾, the lower efficiency of drip irrigation may be due to the fact that the shape of the wet bulb in stratified and heavy soils is not spherical, presenting smaller horizontal diameters. In such soils, higher diameters are expected.



Based on the above, this paper proposes a method to calculate the dimensions of the wet bulb and its dynamics in representative soils of the south of Uruguay, using as the main measurement parameter the water potential (tension) in the soil. For this purpose, a field test was carried out under controlled conditions using soil water potential (tension) as the main measurement parameter to obtain reliable measurements to be used as input to a numerical model. The model was implemented, calibrated and used to identify the optimum irrigation flow rates and frequencies for different scenarios for the considered soils.

2. Materials and methods

The irrigation tests were performed at the National Institute of Agricultural Research's Laboratory (*Instituto Nacional de Investigaciones Agropecuarias* (INIA)), Las Brujas, Canelones, Uruguay; between December 20, 2013 and May 21, 2014. The methodology was based on Provenzano⁽¹³⁾, and complemented by Dabral and others⁽¹⁴⁾; García Petillo and others⁽¹¹⁾⁽¹⁵⁾. A physical model consisting of an instrumented lysimeter was implemented. Then, an irrigation sequence was carried out to measure the dimensions and dynamics of the wet bulb, followed by simulations with a numerical model. The main parameter used in this work was the water potential (tension) in the soil, measured continuously every hour. The drainage phenomenon is strongly dependent on the initial conditions of the system, so once the tensiometers were installed, tension patterns were obtained immediately before starting the irrigation.

2.1 Physical model

A cylindrical watertight lysimeter of 1.20 m diameter and 1.20 m depth was built. These dimensions were considered to ensure that the system boundaries were far enough apart not to affect the wetted zone results. It was installed horizontally to avoid preferential water flows. Then a soil profile representative of the south region of Uruguay was reproduced into the lysimeter, as described later in this section. A surface dripper was installed in the center of the lysimeter to apply the flow rate. Alfalfa was sowed in November in the lysimeter, since it is a reference crop for which direct evapotranspiration data are available (Figures 1 and 2). The experiments began once the crop reached a root development greater than 40 centimeters.



Figure 1. 4 L/h droppers used



Figure 2. Lysimeter with alfalfa planted

The soil considered for this experiment is classified as a typical Brunosol according to the Uruguayan soil classification system⁽¹⁶⁾, and corresponds to a typical Argiudoll according to the Soil Taxonomy classification⁽¹⁷⁾; medium to heavy texture, silty loam. Table 1 presents the description of these soils, predominant in the south and center-south of Uruguay⁽¹⁸⁾.

Table 1. Soil Profile Texture Description

Layer	Depth (cm)	Sand (%)	Silt (%)	Clay (%)	Texture
A	0-25	13	64	23	Silty loam
B	25-65	8	33	59	Silty-clay loam
C	65- +	7	36	57	Silty-clay loam

The methodology to experimentally characterize the soil consisted of plotting the couples (tension-humidity) for all the tensiometers in operation during the testing period, and discarding those that did not present a uniform distribution. Once the tensiometer data had been refined, the parameters of the Van Genuchten⁽¹⁹⁾ equation [3] were fitted: n and m (curve-fitting parameter with $m=1-1/n$), α (empirical parameters), θ_{sat} (saturation humidity) and θ_{res} (residual humidity). The adjusted parameters are shown in Table 2. These parameters were taken as starting values for the calibration in the implementation stage of the numerical model. Then, the parameters were adjusted during calibration, as were the values of hydraulic conductivity.

Table 2. Parameters of the H-Curves (θ)

Depth (cm)	θ_{res} (%)	θ_{sat} (%)	α (m ⁻¹)	n	m
Depth A (0-25)	0.12	0.43	2	1.5	0.33
Depth B (25-65)	0.159	0.474	5	1.5	0.33
Depth C (65- +)	0.18	0.56	5	1.2	0.17

The soil water characteristics obtained with the experimental parameters of the soil water retention curve are presented in Table 3. The bulk density (D_{Ap}), the Field Capacity (CC) was determined as the moisture content measured at -0.01 MPa, and the Permanent Wilt Point (PMP) measured at -1.5 MPa⁽²⁰⁾. For the PMP, values tested in the laboratory with pressure chamber were taken, according to the methodology of Richards⁽²¹⁾.

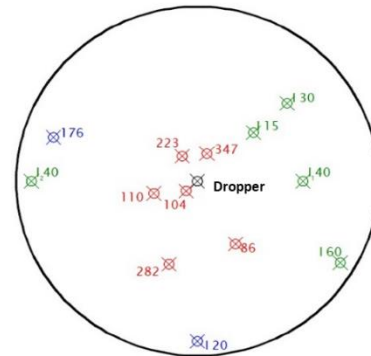
Table 3. Soil water characteristics

Depth (cm)	D _{Ap} (gr /cm ³)	CC (vol-ume)	PMP (vol-ume)	AD (vol-ume)
Depth A (0-25)	1.417	0.320	0.120	0.200
Depth B (25-65)	1.483	0.300	0.159	0.141
Depth C (65- +)	1.603	0.450	0.180	0.270

Nine digital tensiometers connected to a Data Logger (Fig 4) were installed, which recorded continuous measurements every 1 hour during the entire test period. In addition, 4 analogical tensiometers were used as control devices. They were installed at different depths (20cm, 30cm, 40cm, 60cm, 80cm and 100cm) and at different locations in the section (see Figure 3a and b). The equipment was powered

by a 12V, 7Ah battery that was charged by a solar panel installed on site and portable chargers as a backup.

a) Plan



b) Section

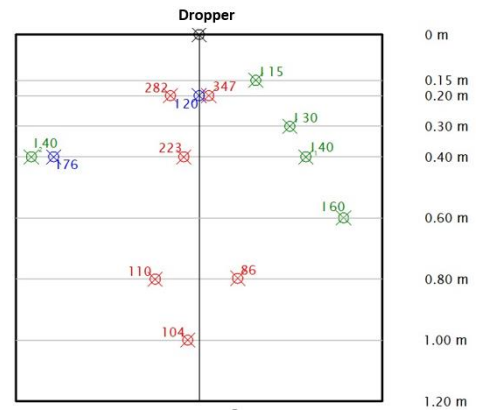


Figure 3. Tensiometers placement scheme

In addition, 4 neutron probe tubes were installed to measure soil water content (H). A probe model CPN 503 (Campbell Pacific Nuclear INC)⁽²²⁾ was used during the period from 1 April to 19 May 2014, where moisture and tension measurements coincided to obtain the experimental data to characterize the soil profile.



Figure 4. 40-cm-long tensiometer and data logger connected to the PC



Figure 5. Neutron Probe model CPN 50

In order to obtain reliable and applicable data for the numerical model, controlled conditions were established, consisting of irrigation and evapotranspiration as the only water inputs to the system, respectively. For this purpose, the lysimeter was installed in a space designed to isolate rainfall, called "Rain-out Shelters" consisting of two "half sheds" which move on a rail closing the roof manually or when rain is detected. The lysimeter was provided with a drain located at the bottom of the system. The outlets were placed 10 cm from the bottom, provided with a tap to measure water outflows. Hourly ETo was calculated according to the Penman-Monteith methodology⁽²³⁾. Data from an automatic weather station (Davis LB model Vantage Pro) located at the site was used for this purpose.

Three irrigation sequences (volume application) consistent with other works reported in the literature⁽¹²⁻¹³⁾⁽²⁴⁾ and with practices and experiences of local producers were programmed: application of 4L/h, each application in times of 1h, 2h and in pulses and two daily applications. Irrigation rate changes were made once the soil reached around -300 hpa. The irrigation system consisted of a pump and emitters in the top center of the lysimeter. The drippers were self-compensating, and the pipes used were 0.5 inch. The pumping system had a pressure of 1 kg/cm².

2.2 Numerical modeling

A numerical model was developed to predict the characteristics of the wetted zone by localized irrigation, in particular the shape of the wet bulb and its dynamics. The code, Code_Bright⁽²⁵⁾, was selected,

which solves thermo-hydro-mechanical problems with 2D and 3D transient flows in saturated and unsaturated soil. The following assumptions were adopted for the model implementation:

- No thermodynamic, soil mechanics and solute transport phenomena are considered. This implies that the equation describing the physical phenomenon to be modeled (conceptual model) is the Richards equation.

Each horizon is considered homogeneous; however, the intrinsic permeability is accepted to vary in the horizontal (radial, r) and vertical (y) directions.

- Hysteresis phenomena were not considered for the wetting and drying cycles of the soil.

The liquid water conservation equation and unsaturated flow were considered for the model. Based on the simplifications of the conceptual model, the type of problem selected in the code is the one that corresponds to the water mass balance where the unknown is PI (liquid pressure), working with the liquid phase and only with the water species (w). The Code_Bright code considers the following expression for the water conservation equation [1] and [2].

$$\frac{\partial(\theta_l^w s_l \phi)}{\partial t} + \nabla \cdot (\mathbf{j}_l^w) = f^w \quad [1]$$

S_l : Degree of saturation of the liquid phase.

(% of pores occupies by water in the liquid state)

θ_l^w : Mass content of water per unit volume in the liquid phase

\mathbf{j}_l^w : Mass flow rate of liquid water

f^w : External water ingress

ϕ : Porosity

$$\mathbf{j}_l^w = -\frac{k \cdot k_{rl}}{\mu_l} (\nabla P_l - \rho_l g) \quad [2]$$

μ^l and ρ^l are the dynamic viscosity, density of water at 20°C

g : gravity

P_l : Relative to atmospheric pressure.

($P_l = 0 = P_{atm}$)

This equation is the Richards equation, which describes the physical phenomena to be modeled (conceptual model).

For the retention curves, the Van Genuchten model was selected. [3]

$$S_0 = \frac{S_l - S_{r1}}{S_{ls} - S_{r1}} = \left(1 + \left(\frac{P_g - P_l}{P} \right)^{\frac{1}{1-\lambda}} \right)^{-\lambda} \quad [3]$$

$$P = P_0 \frac{\sigma}{\sigma_0}$$

P_l : Relative to atmospheric pressure. ($P_l = 0 = P_{atm}$)

P_0 : Measured P at certain temperature $\frac{1}{\alpha}$

σ_0 : Surface tension at temperature in which P_0 was measured

Usually $\sigma_0 = 0,072$ N/m at 20°C

λ : Shape function for retention curve

S_{r1} : Residual saturation

S_{ls} : Maximum saturation

φ_0 : Reference porosity

For intrinsic permeability, the model of Kozeny [4] was used.

$$k = k_0 \frac{\varphi^3 (1 - \varphi_0)^2}{(1 - \varphi)^2 \varphi_0^3} \quad [4]$$

k_0 : Intrinsic permeability referred to φ_0

$(k_{11})_0, (k_{22})_0, (k_{33})_0$: Intrinsic permeability

1st, 2nd, 3rd principal component principal component of the direction respectively

φ_0 : Reference porosity to calculate intrinsic permeability

The Van Genuchten model [5] was used for relative permeability.

$$k_{r1} = \sqrt{S_e} \left(\left(1 - S_e^{1/\lambda} \right)^\lambda \right)^2 \quad [5]$$

$$k_{r1} = \frac{k(h)}{k_{sat}}$$

λ : exponent

S_{r1} : Residual saturation

S_e : Maximum saturation

The domain considered in the model consists of a cylinder of dimensions 0.6 m radius and 1.2 m depth, for which axial symmetry is considered. The dripper (water inlet) is at the point (0,0) of the domain, which represents the center of the real lysimeter. The domain is divided into four bands with depths of 25 cm, 40 cm, 35 cm and 20 cm corresponding to horizons A, B, C and drainage layer, respectively. The model mesh was generated by the program automatically selecting triangular elements. In this case, it was decided to have a denser mesh in the region where the bulb was supposed to develop. Each tensiometer was assigned a node in the generated mesh. A scheme of the domain with the dripper and the position of the tensiometers is shown in Figure 6.

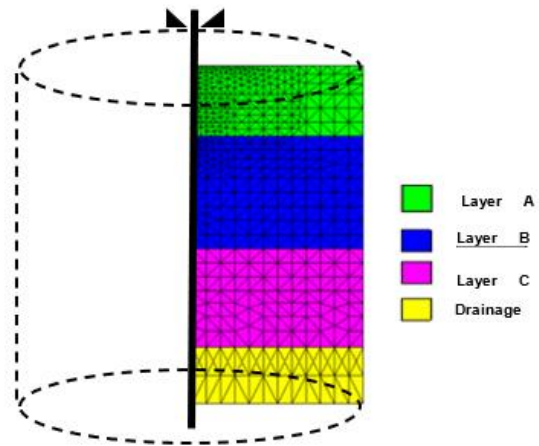


Figure 6. Scheme of the meshed domain and position of the tensiometers associated with the corresponding calculation nodes

The following equation represents the general calculation scheme for boundary conditions. They incorporate von Newman type terms and Cauchy type [6]. In this way, the inputs and outputs at the boundaries are represented in the model by:

$$j_l^w = (w_1^w)^0 j_l^0 + (w_1^w)^0 \gamma_l (P_l^0 - P_l) + \beta_l \left((\rho_l w_1^w)^0 - (\rho_l w_1^w) \right) \quad [6]$$

j_l^w : Water flow rate

w_1^w : mass fraction of solute

P_l : liquid pressure

γ_l = Parameter needed to be $\neq 0$ when P_l is prescribed

ρ_l : liquid density



β_i : Parameter considered only when mass transport is present

Root uptake is an outflow of the system. This was represented by evapotranspiration. Although in the literature⁽⁴⁾⁽²⁶⁻²⁷⁾ there are some models described to represent root absorption, it is difficult to find a model that represents the complexity of this system⁽²⁸⁾. Therefore, root uptake was modeled as water output equal to evapotranspiration distributed in a volume equal to the surface of the lysimeter by a depth of 40 cm. This assumes that the roots were uniformly distributed in this volume and that this was the zone of greatest root activity.

A no-flow condition was applied in the direction perpendicular to the edge of the lysimeter and in the axis of axial symmetry [7] and [8].

$$j_l^w(R, \bar{y}) = (w_1^w)^0 j_l^0 = 0 \quad [7]$$

$$j_l^w(0, \bar{y}) = (w_1^w)^0 j_l^0 = 0 \quad [8]$$

A seepage-type drainage boundary condition was set at the bottom base of the lysimeter. This condition enables drain if and only if the pressure set at the boundary (P_0) in this case set to zero is equal to or less than the pressure of the liquid phase. This is in case there is saturation; otherwise, the flow through the lower boundary of the lysimeter is zero [9].

$$j_l^w(\vec{r}, L) = \begin{cases} j_l^w & \text{si } P_1(\vec{r}, L) \geq 0 \\ 0 & \text{si } P_1(\vec{r}, L) \leq 0 \end{cases} \quad [9]$$

The initial values of the unknowns were assigned in nodes/surfaces on the geometry with constant values. In this case, the only variable to which an initial condition is assigned is the pressure. The surfaces were defined according to the zone influenced by each tensiometer, assigning to it the value measured at the beginning of each test in each tensiometer. As a first approximation, the parameters obtained from the experimental curves for the three soil horizons were fixed and the parameters corresponding to the intrinsic permeability were adjusted, starting from literature values. In a second instance and by means of a manual calibration, the parameters of the curves were varied to reproduce the period in which the soil was irrigated with 4L/h, as shown in Table 5. The calibration parameters were five: α , m , K_0 , r , K_0 , λ .

For the calibration, it was first sought to obtain a single set of parameters to reproduce the three types of applications carried out, however, this was not achieved because it was observed that the soil permeability curves varied as the test time elapsed. This may be due to an incomplete consolidation of the lysimeter soil. In this context, it was decided to calibrate the values of the soil parameters for each irrigation rate period.

Table 4. Irrigation rates considered

Volume application	Q (L/h)	Irrigation time (h)	Daily Application	Jl (kg/s)	Daily volume (L)
4L1h	4	1	1	0.00111	4
4L2h	4	2	1	0.00111	8
4Lp1h	4	1	2	0.00111	8

The Mean Absolute Relative Error coefficient⁽²⁹⁾ was used to evaluate the numerical model. It was calculated as equation [10]:

$$ERMA = \frac{1}{n} \sum_{i=1}^n \frac{|O_i - S_i|}{|O_i|} \quad [10]$$

O_i : values observed in a sample of size "n".

S_i : values calculated by the model in a sample of size "n".

A schematic of the simulated lysimeter and the position of the tensiometers at each node (used for calibration), and the position of the control tensiometers are shown in Figure 7.

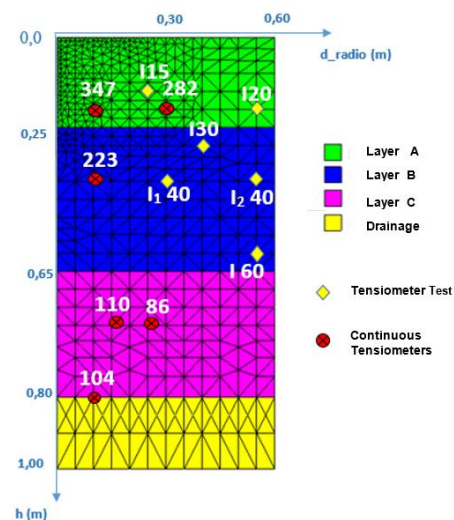


Figure 7. Scheme of the lysimeter mesh with the nodes at the position of the simulated tensiometers

2.3 Numerical simulation

For the simulation of the wet bulb shape, a period of 5 days in January was considered, and the volume and application times of 1 h, 2 h, and 0.5 h and 1 h pulses were evaluated. The initial conditions (and because they are transient phenomena) determine the behavior of the wet bulb dynamics. A typical situation in irrigation management in Uruguay was selected, consisting of an initial condition of soil moisture of 300 hPa in the whole profile.

3. Results

3.1 Model calibration

Table 5 shows the calibration results for the application volume of 4L.

Table 5. Calibration Parameters (4L/h Volume application)

Volume application		4L1h	4L2h	4Lp1h
Horizon A	α (m ⁻¹)	5	5	5
	m	0.33	0.3	0.3
	λ	0.3	0.3	0.3
	Kx	1xe-11	1xe-11	1xe-10
	Ky	1xe-10	1xe-10	1xe-10
Horizon B	α (m ⁻¹)	5	5	5
	m	0.33	0.3	0.3
	λ	0.3	0.3	0.3
	Kx	1xe-12	1xe-12	1xe-12
	Ky	1xe-11	1xe-11	1xe-11
Horizon C	α (m ⁻¹)	5	5	5
	m	0.3	0.3	0.3
	λ	0.4	0.4	0.4
	Kx	1xe-10	1xe-10	1xe-11
	Ky	1xe-11	1xe-11	1xe-11

In Table 6 the ERMA indicates the relative difference of the error made by the model. The following table shows the results of the evaluation coefficients of the numerical model for each tensiometer in each irrigation rate period.

For the present work, acceptable calibration settings were those that obtained an ERMA index of less than 15%.

Figures 8, 9 and 10 compare the model outputs at the positions of the tensiometers whose data were used for the calibration stage for the 3 volume

application proposed (Figures 8, 9 and 10 in Supplementary material).

The difference in the simulation times in each test corresponds to equipment failure events where the Data Logger did not record data. The criterion was to simulate the entire period available with data in each volume application. The error plotted corresponds to the voltage measurement system (+/-5hPa) according to SWT6⁽³⁰⁾.

Table 6. Results of the numerical model evaluation

ERMA (%)						
Volume application	Node					
	347	283	223	110	104	86
4L1h	14.2	3.8	8.0	9.6	7.3	2.4
4L2h	8.4	4.7	8.7	1.2	2.6	2.3
4Lp1h	9.03	6.2	4.4	5.6	ND	4.5

3.2 Radius and depth of the bulbs

Table 7 shows the maximum radius and depths reached by the experimental treatments. An isobaric value of 0.01 MPa was taken as the limit of the wet zone (wet bulb), which corresponds to a soil at field capacity.

Table 7. Radius and maximum depths of calibrated tests

Volume application		4L1h	4L2h	4Lp1h
1 st Application	Rmax (cm)	17	20	17
	h _{Rmax} (cm)	0-25	22	0
	hmax (cm)	50	52	18
End of Range Period	Rmax (cm)	17	20	18
	h _{Rmax} (cm)	30	22	0
	hmax (cm)	50	52	21
Nº of application		6d	1d	6/3 d

3.3 Numerical simulation

Regarding the results of the wet bulb shape simulations, figures 11 to 14 show the evolution of the wetted zone after each application and the time at which the maximum radius was reached once



irrigation was finished each day (Figures 11 to 14 in Supplementary material).

4. Discussion

From the previous figures, a good adjustment is observed in the tensiometers placed in the center of the lysimeter, that is, below the dripper, while the values of the tensiometers placed below 60 cm show a greater deviation. This can be noticed for all irrigation rates. At the same time, as the application volume increased, better adjusted calibrations were achieved.

For tensiometers placed below 60 cm, the model presented lower quality in the adjustments. The model tends to equilibrium, not capturing rapid water arrivals, which can be associated with the entry of water through preferential routes in soils with macropores, probably due to the wetting-drying cycles to which the soil was subjected⁽³¹⁻³²⁾. This effect is not noticeable in the upper part of the lysimeter because the area associated with macroporosity tends to decrease with depth⁽³³⁾. This is why these oscillations are not associated with the different irrigation applications, which can be observed in the surface tensiometer graphs. This indicates that the water that reaches the deeper strata arrives very slowly and is distributed in the area.

4.1 Parameters of the retention curves

For the parameters of the retention curves, they never reached values typical of clay soils as cited in the literature⁽²⁾⁽²⁰⁾⁽³⁴⁻³⁵⁾. This can be explained as we are dealing with structural phenomena of macroporosity, where the hydrodynamic response of the soil (on a macro scale) resembles parameters of coarser textured soils. Figures 15, 16 and 17 show the comparison of the retention curves in their evolution over time of the irrigation treatments (using the sets of parameters calibrated in the model) vs. the theoretical curve for each horizon of the profile.

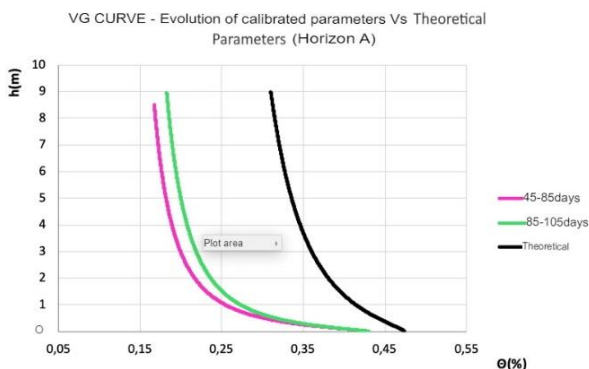


Figure 15. Comparison of retention curves, their evolution in test time and theoretical for Horizon A

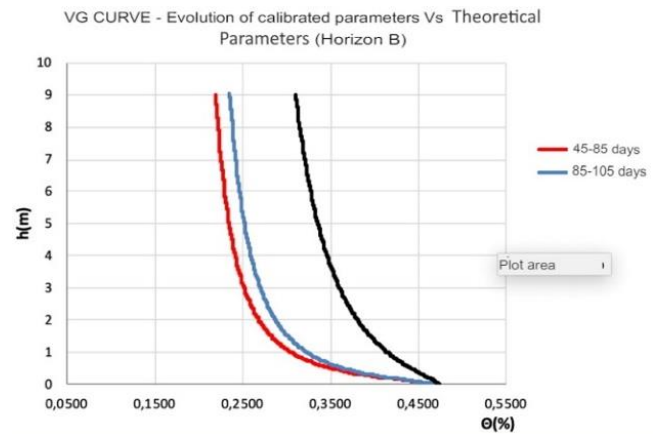


Figure 16. Comparison of retention curves, their evolution in test time and theoretical for Horizon B

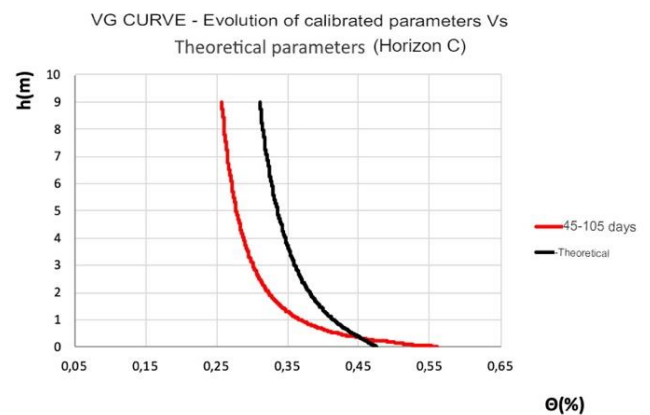


Figure 17. Comparison of retention curves, their evolution over test and theoretical time for Horizon C

4.2 Forecasting the wet bulb shape

Regarding the results for the measurements of radius and depth of the bulbs, the dimensions of the wet bulbs in clay soils in the literature⁽³⁶⁻³⁸⁾ should be between 30 and 40 cm for maximum radii and depths less than 40 cm. As can be seen in Table 8, the trend of the maximum radii and calibrated depths are lower for the former and higher for the latter, compared to those reported in the literature.

Table 8. Theoretical values for clayey soils

Theoretical Parameters	
α (m ⁻¹)	1,4
m	0,24
λ	0,3
Kx	1xe ⁻¹³
Ky	1xe ⁻¹⁵

Regarding the number of applications, it is interesting to note that for all cases, in the successive applications, the radii grow as the initial conditions are

varied after each application. This suggests that it is necessary not to let the soil dry out and to look for an optimal efficiency range of moisture/tension in which irrigation should be applied. Moreover, such management avoids transformations at the structural level of the soil, such as cracks and changes in the porosity, which decrease the water holding capacity of the soil and, therefore, increase percolation losses.

The model adequately represents the dynamics of the wet bulb at a macro scale; however, it does not represent the existence of phenomena where porosities are present at different scales, e.g. macropores, preferential paths, since the numerical model used did not conceptually take this phenomenon into account. In this case, the porosity is represented by a single value per soil type, simply having established the parameters of the corresponding water retention curves. In any case, the results of the simulations for the radii were lower than those established by the literature⁽³⁸⁾ for the soils used in this work, as well as the greater depths.

Regarding pulse irrigation, we can observe that although the radius is reduced, so is the depth that reaches the wet zone in all treatments. It can be observed that as the daily volume is distributed in more applications per day —e.g., the irrigation time is distributed in each application—, greater reductions in depth are achieved.

As for the comparison of the bulb dimensions, it can be observed that the radii reached in the different simulations of the irrigation volume application were always smaller than those presented in the bibliography, and the opposite is the case with the depth reached by the bulb. As an example, Table 9 shows the comparison between literature values for clay soils and those obtained by the simulations for similar volume applications. This is explained by the fact that in most cases the soil properties are based on the description of the texture, giving little weight to the structure. This is evidence of structural phenomena of the clays of southern Uruguay that impose a change in the conceptual model of single porosity, as mentioned in previous paragraphs.

Table 9. Comparison of literature values and those obtained from simulations

	R max (cm)			H max (cm)	
	Simulations	Bresler ⁽³⁹⁾	Karmelli and others ⁽³⁵⁾	Simulations	Bresler ⁽³⁹⁾
4L/h 1 hour of irrigation	16	25-30	80	32	15
4L/h 2 hours of irrigation	25	35	100	43	20

The effect of preferential paths (fissures) in this type of soil is potentially more important the drier it is, weighing structural and macro-scale phenomena over textural ones. The numerical model does not consider changes in porosity or mechanical phenomena, so an alternative to improve the model fit could be the incorporation of other phenomena such as double porosity.

It is understood that to improve this aspect of the model, macro structural phenomena should be incorporated into the conceptual model, which implies abandoning the concept of constant porosity as a soil property and activating the simulation of soils with double porosity in the numerical model. At the same time, parameters of the Van Genuchten curve(s) should be considered, where maintaining the tension —i.e., the main measured variable— forces the soil to lose more water.

5. Conclusions

This paper presents the calibration of a model for heavy and stratified soils with a silty loam and silt-

clay loam texture, typical of southern Uruguay. The model fits more adequately in the upper strata ($h < 60\text{cm}$) and has limitations in the deeper strata, underestimating the vertical drainage and overestimating the horizontal distribution.

Through the calibrated model it was possible to evaluate the influence of different irrigation applications on the shape of the wet bulb in stratified and heavy soils. Contrary to accepted literature, the horizontal diameters of the wet bulb are consistently smaller. Our findings reveal that understanding the initial soil stress/moisture conditions is critical to effective design. Pulse irrigation promises to reduce percolation losses, with reductions of up to 11% in two daily applications and up to 23% in four daily applications. To optimize design strategies, it is recommended to maintain soil moisture within a specific range to counter macroporosity-related deep percolation losses. Working with lower flow rates can improve efficiency, although it can result in smaller wet front radii and reduced maximum wet depth. Also, achieving overlap of wetting bulbs through proximity of drippers offers an effective



technique. The concept of distributing the daily irrigation volume over multiple applications also emerges as a viable strategy to minimize percolation losses.

Acknowledgements

I would like to express my sincere gratitude to ANII for generously granting me the funds necessary to carry out this project. Thanks to their support, I was able to allocate adequate time and resources to conduct thorough research.

I must also acknowledge the invaluable contribution of the dedicated staff at INIA, who oversees the irrigation area. Their collaboration and provision of essential resources within the institution were instrumental in successfully executing the experimental stage of this project.

Transparency of data

Data not available: The data set that supports the results of this study is not publicly available.

Author contribution statement

Teresa Sastre: Design and execution of the physical experiment. Development of the mathematical model and calibration. Analysis of results. Writing of the paper.

Luis Silveira: Support in the design and execution of the physical experiment. Analysis of results. Collaboration in writing the paper.

Pablo Gamazo: Support in the development of the mathematical model and calibration. Analysis of results. Collaboration in writing the paper.

References

1. Kijne JW. Descubrir el potencial del agua para la agricultura. Roma: FAO; 2003. 62p.
2. Rodrigo Lopez J, Hernandez Abreu JM, Perez Regalado A, Gonzalez Hernandez JF. Riego Localizado. Madrid: Mundi-Prensa; 1992. 416p.
3. Varshney RS. Modern Methods of Irrigation. GeoJurnal. 1995;35:59-63.
4. Coelho FE, Or D. Root distribution and water uptake patterns of corn under surface and subsurface drip irrigation. Plant Soil. 1999;206:123-36.
5. Mmolawa K, Or D. Water and solute dynamics under a drip irrigated crop: experiments and analytical model. Trans ASAE. 2000;43:1597-608.
6. Cook FJ, Fitch P, Thorburn PJ, Charlesworth PB, Bristow KL. Modelling trickle irrigation: comparison of analytical and numerical models for estimation of wetting front position with time. Environ Model Softw. 2006;21:1353-9.
7. Levin I, Van Rooyen PC, Van Rooyen FC. The effect of discharge rate and intermittent water application by trickle irrigation on soil moisture distribution pattern. Soil Sci Soc Am J. 1979;43(1):8-16.
8. Molavi A, Sadraddini A, Nazemi AH, Fakheri Fard A. Estimating wetting front coordinates under surface trickle irrigation. Turk J Agric For. 2012;36:729-37.
9. Souza CF, Folegatti MV, Or D. Distribution and storage characterization of soil solution for drip irrigation. Irrig Sci. 2009;27:277-88.
10. Abrat G, Puig-Bargués J, Duran-Ros M, Barragán J, Ramírez de Cartagena F. Drip-Irrigation: computer software to simulate soil wetting patterns under Surface drip irrigation. Comput Electron Agric. 2013;98:183-92.
11. García Petillo M. Análisis crítico del método de riego por goteo en las condiciones del Uruguay. Agrociencia. 2010;14(1):36-43. Doi: 10.31285/AGRO.14.638.
12. García Petillo M. Respuesta a diferentes manejos del riego y balance hídrico de un huerto de cítricos [doctoral's thesis]. Valencia (ES): Universidad Politécnica de Valencia, Escuela Técnica Superior de Ingenieros Agrónomos; 2002. 194p.
13. Provenzano G. Using Hydrus-2D Simulation Model to evaluate wetted soil volume in subsurface drip irrigation systems. J Irrig Drain Eng. 2007;133(4):342-9.
14. Dabral PP, Pandey PK, Pandey A, Singh KP, Sanjoy Singh M. Modelling of wetting pattern under trickle source in sandy soil of Nirjuli, Arunachal Pradesh (India). Irrig Sci. 2012;30:287-92.
15. García Petillo M, Hayashi R, Silveira L, Sastre T, Puppo L, Morales P. Proyecto 10035P Fondo Profesor Clemente Estable: Análisis de las dimensiones del bulbo húmedo bajo riego localizado en los suelos del Uruguay y ajuste de un modelo matemático: informe final. Montevideo: DICyT; 2008. 29p.
16. Altamirano A, Duran A, Da Silva H, Echevarría A, Puentes R, Panario D. Carta de reconocimiento de suelos del Uruguay. Montevideo: MAP; 1976. 96p.

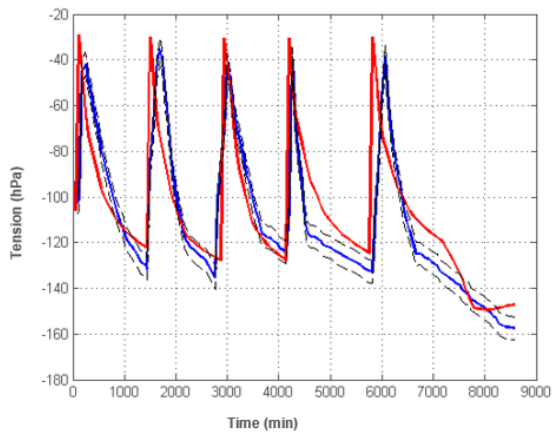


17. Soil Survey Staff. Soil taxonomy: a basic system of soil classification for making and interpreting soil surveys. 2nd ed. Washington: USDA; 1999. 869p.
18. Durán A, García Préchac F. Suelos del Uruguay: origen, clasificación, manejo y conservación. Montevideo: Hemisferio Sur; 2007. 2v.
19. Van Genuchten MT. A closed form equation for predicting the hydraulic conductivity of unsaturated soils. *Soil Sci Soc Am J.* 1980;44(5):892-8.
20. Pizarro F. Riegos localizados de alta frecuencia (RLAF) goteo, microaspersión y exudación. 2^a ed. Madrid: Mundi-Prensa; 1990. 471p.
21. Richards LA. Methods of measuring soil moisture tension. *Soil Sci.* 1949;68(1):95.
22. Campbell Pacific Nuclear Inc. Operating manual 503DR. Durham: InstroTek. Operating; 2013. 47p.
23. Allen RG, Pereira LS, Raes D, Smith M. Evapotranspiración del cultivo: guías para la determinación de los requerimientos de agua de los cultivos. Roma: FAO; 2006. 298p.
24. Lopez Canteñs G, Herrera Puebla J, Ostos Santoa A, Lizarraga Mendiola L, Hernandez-Avila J. Aplicación de modelos matemáticos para la obtención de la curva de retención de humedad del suelo. *Rev latinoam recur nat.* 2010;6(1):44-50.
25. Olivella S, Gens A, Carrera J, Alonso EE. Numerical formulation for a simulator (Code-Bright) for the coupled analysis of saline media. *Eng Comput.* 1996;13(7):87-112.
26. Clothier BE, Green SR. Roots: the big movers of water and chemical in soil. *Soil Sci.* 1997;162:696-700.
27. Simunek J, Sejna M, Van Genuchten MT. The Hydrus-2D software package for simulating two dimensional movement of water, heat, and multiple solutes in variably saturated media. Version 2.0. Riverside: U S Salinity Laboratory; 1999. 225p.
28. Mmolawa K, Or D. Root zone solute dynamics under a drip irrigation: a review. *Plant Soil.* 2000;222:163-90.
29. Wallach R, Li Y, Cohen Y. The role of soil hydraulic conductivity on the spatial and temporal variation of root water uptake in drip irrigated corn. *Plant Soil.* 2002;243:131-42.
30. AT Delta-T Devices Ltd. SWT6, SWT4, SWT4R User Manual. London: Delta-T Devices; 2009. 52p.
31. Jarvis NJ. The MACRO model (Version 3.1): technical description and sample simulations. Uppsala: Swedish University of Agricultural Sciences; 1994. 51p.
32. Rubio C, Llorens P, Van Genuchten MT. Modelización del flujo transitorio en suelo franco-limoso utilizando Hydrus 1D. In: Samper J, Paz A, editors. Estudios de la Zona No Saturada. Vol. 7, Estudios de zona no saturada del suelo. La Coruña: Universidade da Coruña; 2005. pp. 257-61.
33. Lexow C. Curso Hidrodinámica de la Zona no Saturada. Santa Rosa: Universidad de la Pampa; 2006. 121p.
34. Zazueta FS. Micro Irrigación. México: ICFA; 1992. 212p.
35. Mallants D, Mohanty BP, Vervoort A, Feyen J. Spatial analysis of saturated hydraulic conductivity in a soil with macropores. *Soil Technol.* 1997;10(2):115-31.
36. Karmelli D, Peri G, Todes M. Irrigation systems: design and operation. Oxford: Oxford University Press; 1985. 187p.
37. Quezada C, Venegas A, García H, Ocampo J. Frecuencia de reposición Hídrica en Olivos bajo riego por goteo en un suelo franco-arcilloso. *Agro Sur.* 2005;33(2):74-86.
38. Keller J, Bliesner R. Sprinkle and trickle irrigation. New York: Van Nostrand Reinhold; 1990. 652p.
39. Bresler E. Trickle drip irrigation: principles and applications to soil-water management. *Adv Agron.* 1977; 29:344-93.

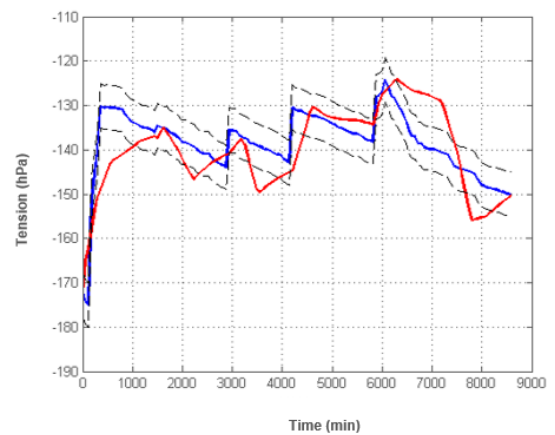


Supplementary material

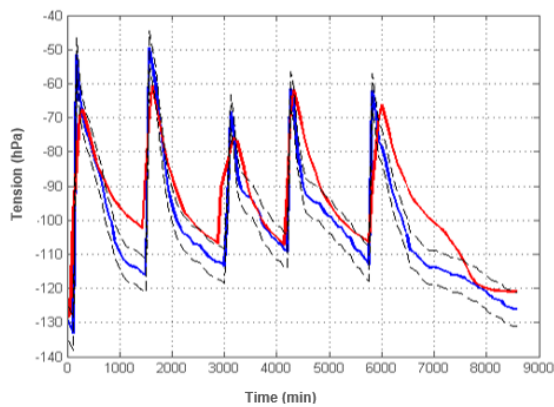
Node 347 (0.1; 0.2)



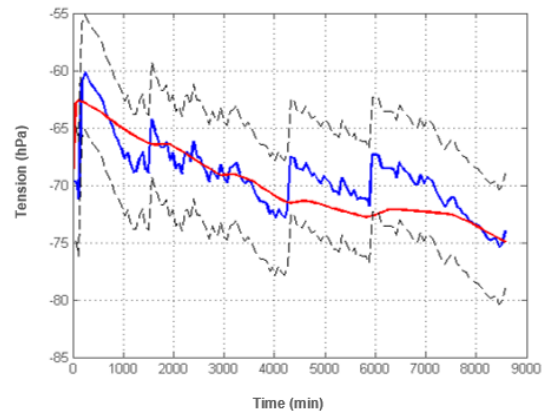
Node 282 (0.3; 0.2)



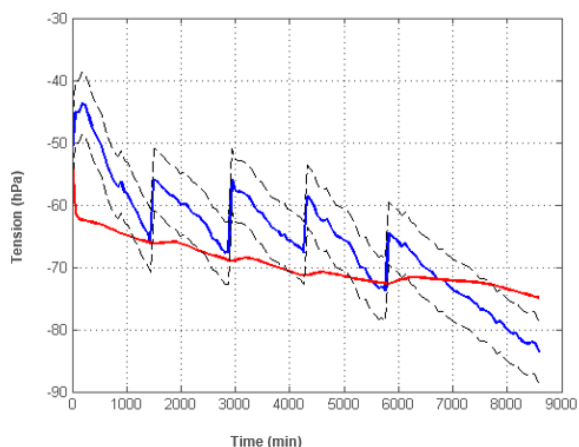
Node 223 (0.1; 0.4)



Node 86 (0.25; 0.8)



Node 110 (0.1; 0.8)

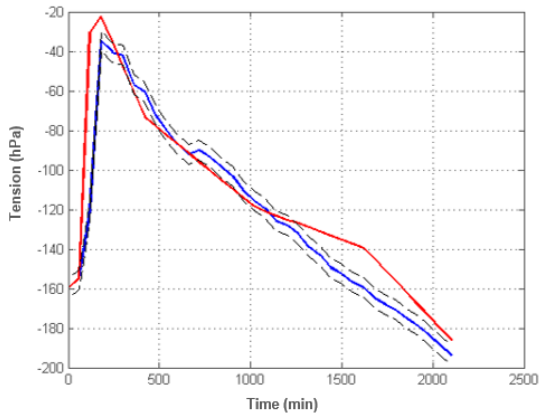


Observed —
 Model —
 Error + - - -
 Error- - · -

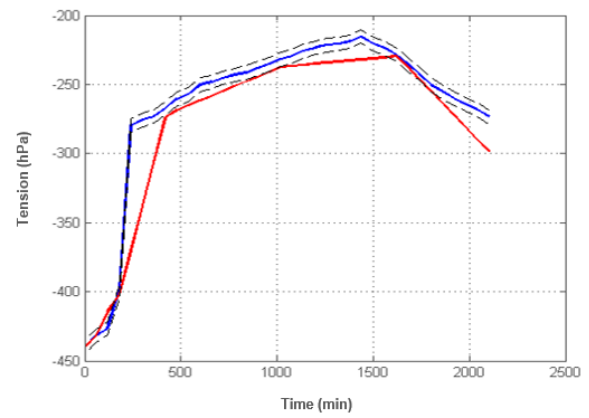
Figure 8. Observed and modeled stress for a flow rate of 4 L per day in 1 daily application of 1 hour (4L1h). For each node, the coordinates of the associated tensiometer (r, h) are indicated in parentheses, where r is the radius and h is the depth. Calibration period 143 hours



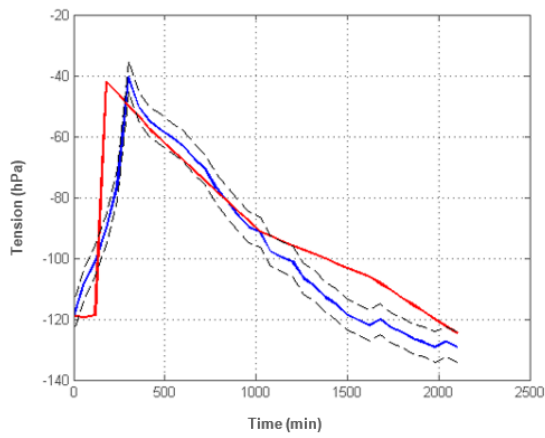
Node 347 (0.1; 0.2)



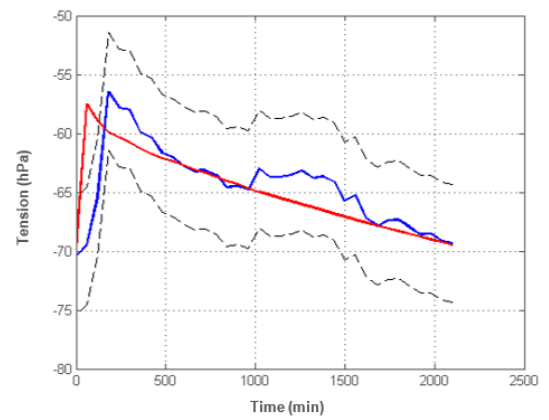
Node 282 (0.3; 0.2)



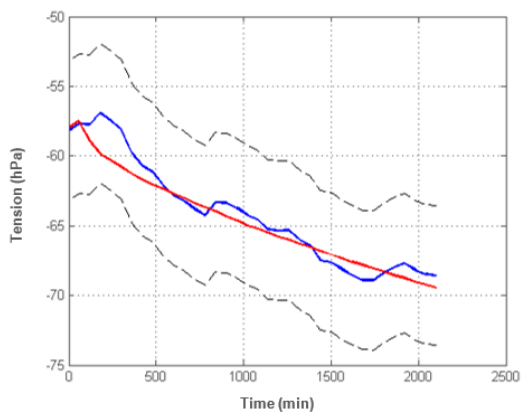
Node 223 (0.1; 0.4)



Node 86 (0.25; 0.8)



Node 110 (0.1; 0.8)

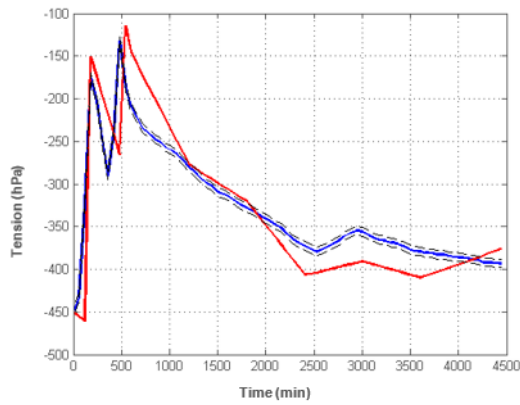


Observed ———
Model ———
Error + - - - -
Error- - - - -

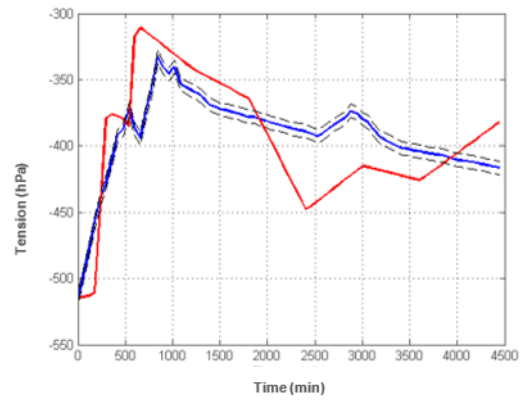
Figure 9. Observed and modeled voltage for a flow rate of 4 L per day in 1 daily application of 2 hours (4L2h). Calibration period 35 hours



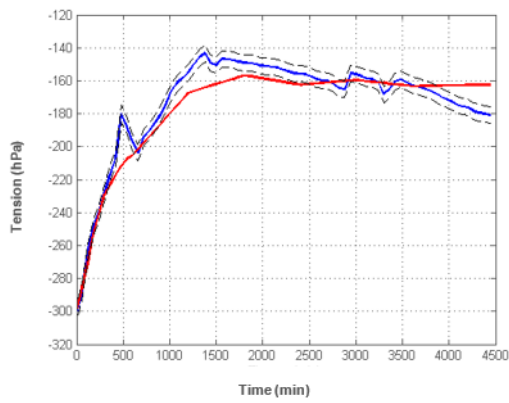
Node 347 (0.10; 0.2)



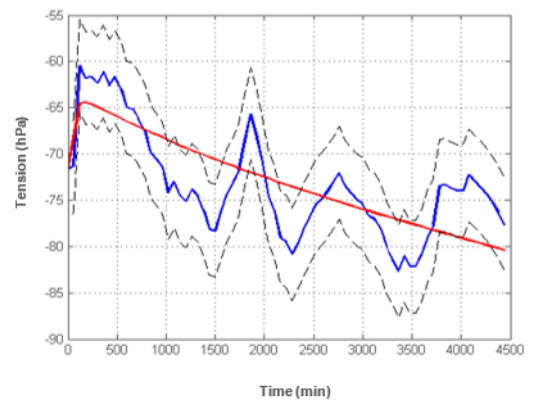
Node 282 (0.3;0.2)



Node 223 (0.1; 0.4)



Node 86 (0.25; 0.8)



Node 110 (0,1; 0,8)

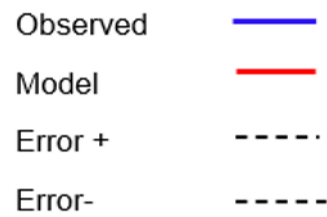
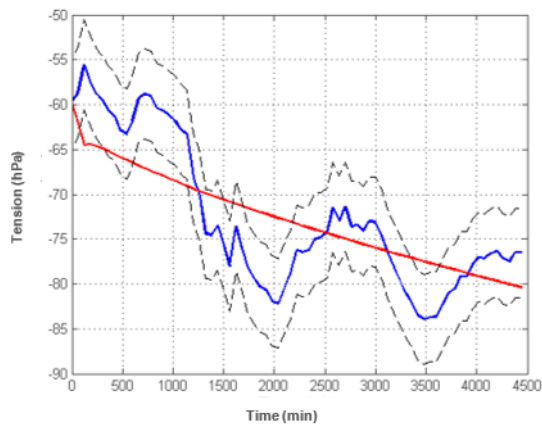


Figure 10. Observed and modeled voltage for a flow rate of 4 L per day in 2 daily applications of 1 hour (4Lp1h). Calibration period 35 hours

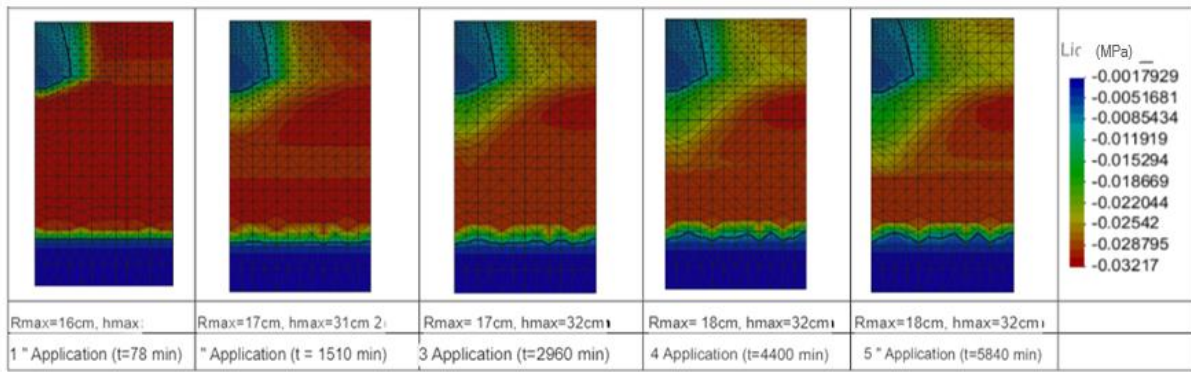


Figure 11. Volume application 4L 1h (one application)

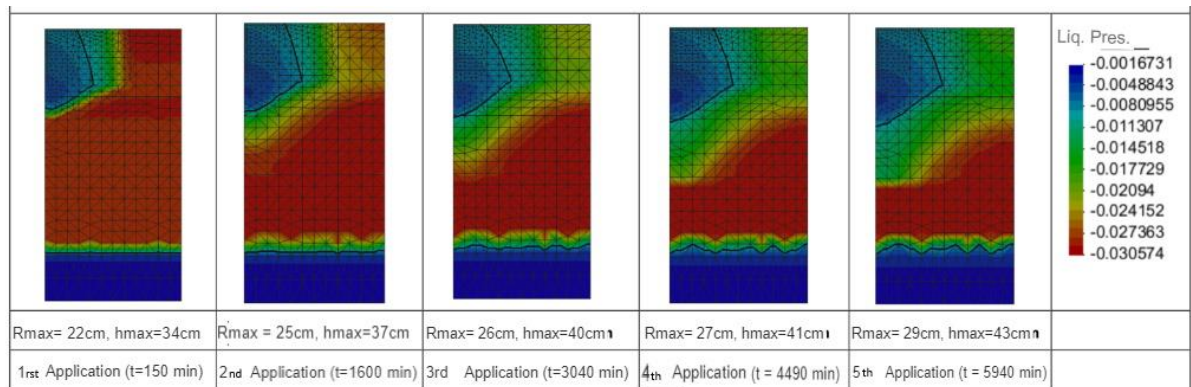


Figure 12. Volume application 4L 2h (one application)

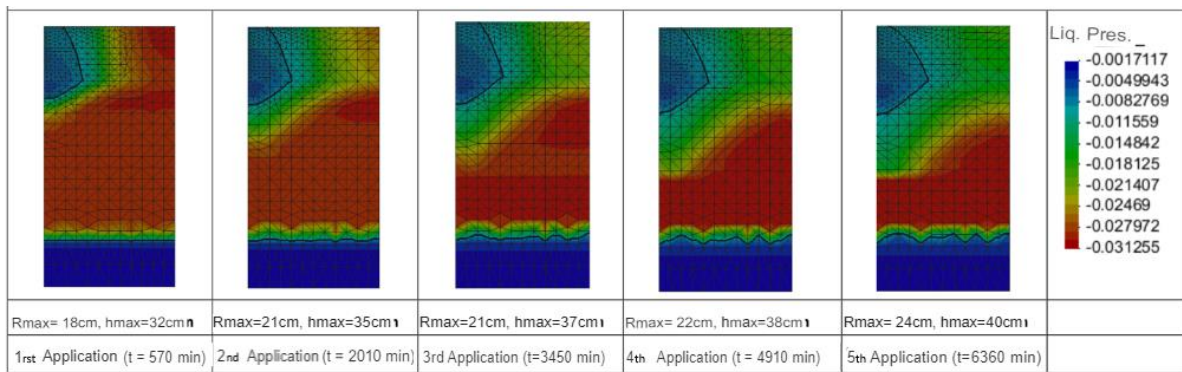


Figure 13. Volume application 4L p 1h (two applications per day)

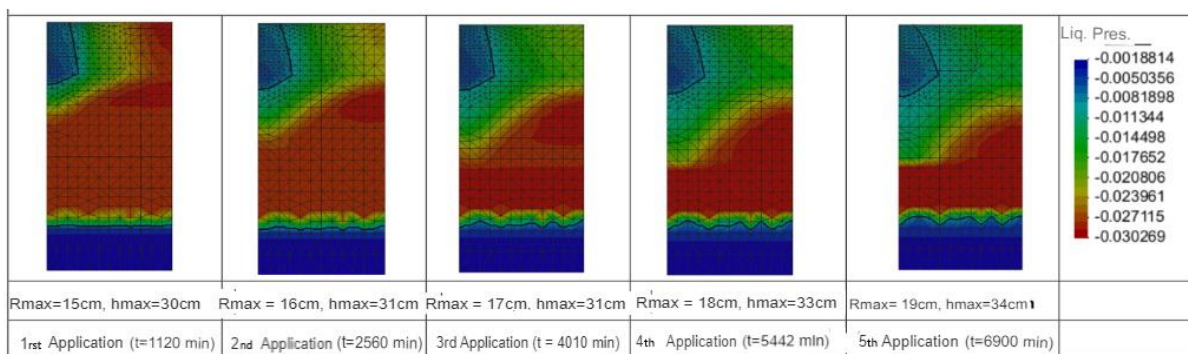


Figure 14. Volume application 4L p 0.5h (four applications per day)